Enhancing Sensitivity and Selectivity of Long-Period Grating Sensors using Structure-Switching Aptamers Bound to Gold-Doped Macroporous Silica Coatings

ARTICLE *in* ANALYTICAL CHEMISTRY · SEPTEMBER 2011

Impact Factor: 5.64 · DOI: 10.1021/ac2020432 · Source: PubMed

5 AUTHORS, INCLUDING:

Carmen Carrasquilla
McMaster University
9 PUBLICATIONS **71** CITATIONS

SEE PROFILE

analytical chemistry

ARTICLE

pubs.acs.org/ac

Enhancing Sensitivity and Selectivity of Long-Period Grating Sensors using Structure-Switching Aptamers Bound to Gold-Doped Macroporous Silica Coatings

Carmen Carrasquilla,[†] Yao Xiao,[‡] Chang Qing Xu,[‡] Yingfu Li,[†,§] and John D. Brennan*[,†]

[†]Department of Chemistry and Chemical Biology, McMaster University, Hamilton, Ontario, Canada, L8S 4M1

[‡]Department of Engineering Physics, McMaster University, 1280 Main Street West, Hamilton, Ontario, Canada, L8S 4L7

[§]Department of Biochemistry and Biomedical Sciences, McMaster University, Hamilton, Ontario, Canada, L8N 3Z5

Supporting Information

ABSTRACT: High surface area, sol−gel derived macroporous silica films doped with gold nanoparticles (AuNP) are used as a platform for high-density affinity-based immobilization of functional structure-switching DNA aptamer molecules onto Michelson interferometer long-period grating (LPG) fiber sensors, allowing for label-free detection of small molecular weight analytes such as adenosine triphosphate (ATP). The high surface area afforded by the sol−gel derived material allowed high loading of DNA aptamers, while the inclusion of gold nanoparticles within the silica film provided a high refractive index (RI) overlay, which is required to enhance the sensitivity of the LPG sensor according to our numerical simulations. By using a structure-switching aptamer construct that could release an oligonucleotide upon binding of ATP, the effective change in RI was both enhanced and inverted (i.e., binding of ATP caused a net reduction in molecular weight and refractive index), resulting in a system that prevented signals originating from nonspecific binding. This is the first report on the coupling of aptamers to LPG fiber sensors and the first use of high RI AuNP/silica films as supports to immobilize biomolecules onto the LPG sensor surface. The dual functionality of such films to both improve binding density and LPG sensor cladding refractive index results in a substantial enhancement in the sensitivity of such sensors for small molecule detection.

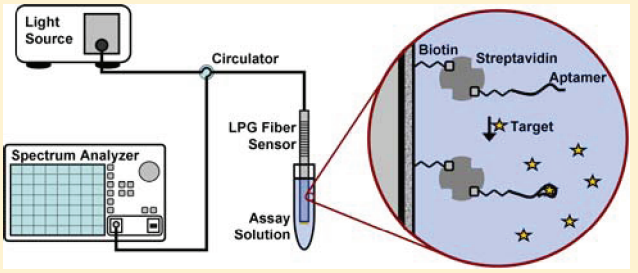

Label-free optical biosensors have gained popularity in recent years owing to the ability to avoid the need for fluorescence or other labeling of biomolecules or analytes.[1,2] One of the most widely employed label-free sensors utilizes surface plasmon resonance (SPR), which is based on the change in the resonance angle upon binding of species to a suitably modified gold surface, or alternatively, the change in reflected intensity upon binding when working at a fixed incidence angle.[3] However, SPR sensors are not easily adapted to fiber-optic sensing platforms, and the working wavelength of the SPR biosensor is not usually in the standard optical communication wavelength, which increases cost.

In recent years there has been an increasing number of reports on label-free fiber-optic biosensors, usually based on fiber Bragg grating (FBG)[4−6] or long-period grating (LPG)[7−9] configurations. The FBG biosensor usually works in a reflection mode and is based on changes in the Bragg wavelength before and after binding of target molecules. The LPG biosensors can also operate in the transmission mode, as the propagation of the evanescent wave into the cladding modes makes the sensor sensitive to changes in the ambient refractive index (RI) in the vicinity of the fiber cladding, measured by shifts in the wavelength of the transmission attenuation bands.[10,11] Moreover, LPG biosensors can function as in-fiber Michelson interferometers through the addition of a mirror at the distal end of the fiber sensor that reflects the copropagating core and cladding modes back to the LPG, resulting in narrow interference fringes within the original attenuation bands that have greater sensitivity to changes in external RI.[12,13] Nevertheless, significant optimization is needed to maximize the RI of the cladding in order to maximize the sensitivity of the LPG biosensor.[14,15]

Previous studies have utilized high RI overlays such as Langmuir−Blodgett thin films[16] or polymeric cladding films with entrapped silver nanoparticles[17] to increase the RI of the cladding, and these were shown to improve the sensitivity of the LPG sensors for detection of changes in ambient RI. However, these films were not amenable to subsequent binding of biomolecules, limiting their utility for biosensing applications. Mesoporous sol−gel derived materials have also been shown to enhance the RI and sensitivity of LPG fibers,[18] and can be prepared with chemically selective species to enhance selectivity.[19] Our group has recently demonstrated the use of high surface area macroporous sol−gel derived silica as a support to immobilize

Received: August 4, 2011
Accepted: September 15, 2011
Published: September 27, 2011

biomolecules, with binding density being 6−10-fold greater than is achieved on planar glass surfaces.[20] We have also reported on the development of sol−gel derived films that were doped with gold nanoparticles (AuNP), and on the ability to grow such particles within the silica film using either conventional reducing agents or enzymatically catalyzed reactions to control particle growth.[21] Therefore, we hypothesized that a combination of macroporous silica films for high density binding of biomolecules and entrapped AuNP to provide a high RI cladding would provide a major increase in the sensitivity of LPG fiber-optic biosensors.

In this paper, we describe the use of AuNP-doped macroporous sol−gel derived films as high surface area, high RI supports for immobilizing structure-switching DNA aptamers onto LPG fiber sensors to allow for high sensitivity detection of the model analyte adenosine 5′-triphosphate (ATP, MW = 507 Da). Aptamers, which are single-stranded nucleic acids that can fold into distinct structures and function as receptors for target molecules, were chosen for this study since they can be generated by in vitro selection for virtually any target of interest[22−24] and have been selected for a number of diverse analytes, including proteins, small metabolites and cells.[24−26]

Thin films were formed by dipcasting of a poly(ethylene glycol) (PEG) doped sodium silicate solution onto the surface of LPG interferometer optical fibers, followed by growth of AuNP within the resulting macroporous silica films.[21,27−30] Following film formation, the silica surface was functionalized to allow binding of biotinylated structure-switching DNA aptamers to the surface. These were then hybridized to cDNA strands containing a quencher moiety (QDNA) to produce a species that could be liberated upon binding of ATP. Introduction of target analytes to this surface induces a conformational change that causes dehybridization of the QDNA strand and produces a large change in RI.[31] The data are compared to cases where immobilization is done directly onto the optical fiber or onto macroporous silica materials without entrapped AuNP, as well as to cases where QDNA strands are not present prior to addition of ATP. These studies demonstrate the enhancement of sensitivity that is obtained using an optimized high RI silica film in conjunction with a strand displacement assay.

EXPERIMENTAL SECTION

Chemicals. Modified oligonucleotides were chemically synthesized by Integrated DNA Technologies (Coralville, IA) and purified by HPLC. Streptavidin, 10 kDa poly(ethylene glycol) (PEG), 3-(aminopropyl)triethoxysilane (APTES), biotin, *N*-(3-dimethylaminopropyl)-N′-ethylcarbodiimide hydrochloride (EDC), *N*,*N*′-disuccinimidyl carbonate (DSC), gold(III)chloride trihydrate (99.9+% metal basis), (tri)sodium citrate dihydrate, and Dowex 50 × 8−100 cation exchange resin were obtained from Sigma-Aldrich (Oakville, ON). Adenosine 5′-triphosphate (ATP), cytosine 5′-triphosphate (CTP), guanosine 5′-triphosphate (GTP) and uridine 5′-triphosphate (UTP) were purchased from Fermentas Life Sciences (Burlington, ON). Sodium silicate solution (SS solution, ultrapure grade, ∼14% Na_2O, ∼29% silica) was purchased from Fisher Scientific (Pittsburgh, PA). Water was purified with a Milli-Q Synthesis A10 water purification system. All other chemicals and solvents were of analytical grade and were used as received.

Bipartite structure-switching aptamers for the detection of ATP were prepared using the following sequences. The bold nucleotide designates the location of a covalently bound fluorescein label (F) in the construct and the italicized nucleotides designate the quencher-DNA binding region for the fluorescence reporter construct of this structure-switching aptamer.

ATP aptamer: 5′-biotin-TTTTTTTTTT**T**FT*CACTGACCTG*-*GGGGAGTATTGCGGAGGAAGGT*-3′,

ATP aptamer quencher-DNA (QDNA): 5′-*CCCAGGTCAGTG*-dabcyl-3′,

Thrombin aptamer quencher-DNA (THR-QDNA): 5′-*CCAACCACAGTG*-dabcyl-3′.

Procedures. *Preparation and Growth of AuNP.* The citrate-capped gold nanoparticles (AuNP) were prepared as described elsewhere.[21,32−34] Briefly, 7.89 mg gold(III)chloride was diluted in 20 mL of water in a round-bottom flask previously cleaned with aqua regia. After bringing the gold chloride solution to a boil with stirring, 2 mL of a 1.14% (w/v) sodium citrate solution was added as a reducing agent. After cooling for 3−4 h, the resulting solution of AuNP had a mean diameter of 13 nm as measured by absorbance at 521 nm.[35] This solution was mixed with the buffer that was used for preparing the sol−gel derived films in order to coat the interferometer arm of the LPG fiber sensors (described below).

Once the AuNP-doped sol−gel derived films had gelled and aged on the LPG fiber sensors, the AuNP were enlarged by fiber immersion in a 10 mM gold chloride solution for 1 h, followed by addition of a 1.14 (w/v) solution of sodium citrate and rinsing in buffer to remove excess gold chloride solution. AuNP-doped sol−gel derived films were also made in microwell plates in order to assess the particle growth upon addition of a gold chloride solution overlay, by measuring the shift in the absorbance maximum. Absorbance spectra were recorded from 450−650 nm using a M1000 platereader at a scan rate of 200 nm·min^{-1}.

Preparation of Sol−Gel Derived Films and Fiber Coating. Buffer solutions were prepared by mixing an equal volume of buffer (100 mM HEPES·NaOH; pH 7.6) with a solution containing 10.0% (w/v) 10 kDa PEG in water. For AuNP-doped buffer solutions, 200 mM HEPES·NaOH at pH 7.6 with 20.0% (w/v) 10 kDa PEG was mixed with the AuNP solution described above in a 1:1 (v/v) ratio prior to combining with the sol−gel precursor. Sodium silicate (SS) solutions were prepared as described elsewhere,[36] by diluting 2.6 g of a stock SS solution to 10 mL with water, mixing the solution with 5.5 g DOWEX to bring the pH of the SS solution to ∼4, and then filtering this solution through a Buchner funnel to remove the resin followed by further filtration through a 0.45 μM membrane syringe filter to remove any particulates in the solution. This solution was combined with the PEG-doped (or PEG and AuNP-doped) buffer solutions in a 1:1 (v/v) ratio inside test tubes into which 40 mm of cleaned SMF-28 fibers (soaked in 1N NaOH for 1 h and rinsed with ethanol) were mechanically dipcast at a withdrawal rate of 12 mm·min^{-1}.

The distal end of the silica film-coated fiber was also coated with a flat gold mirror composed of 20 nm Cr and 300 nm Au by the e-beam evaporation technique (thickness was measured directly by the electron beam deposition instrument when applying these layers on the fibers), prior to dipcasting in the silica sol, such that the sensing head could operate in reflection mode as an interferometer. Silica coated fibers were suspended in air for 4−6 h in order to allow for silica gelation and aging prior to any testing.

Characterization of Sol−Gel Derived Films. In order to characterize the refractive index and thickness of the sol−gel derived silica film, ellipsometry measurements were performed on

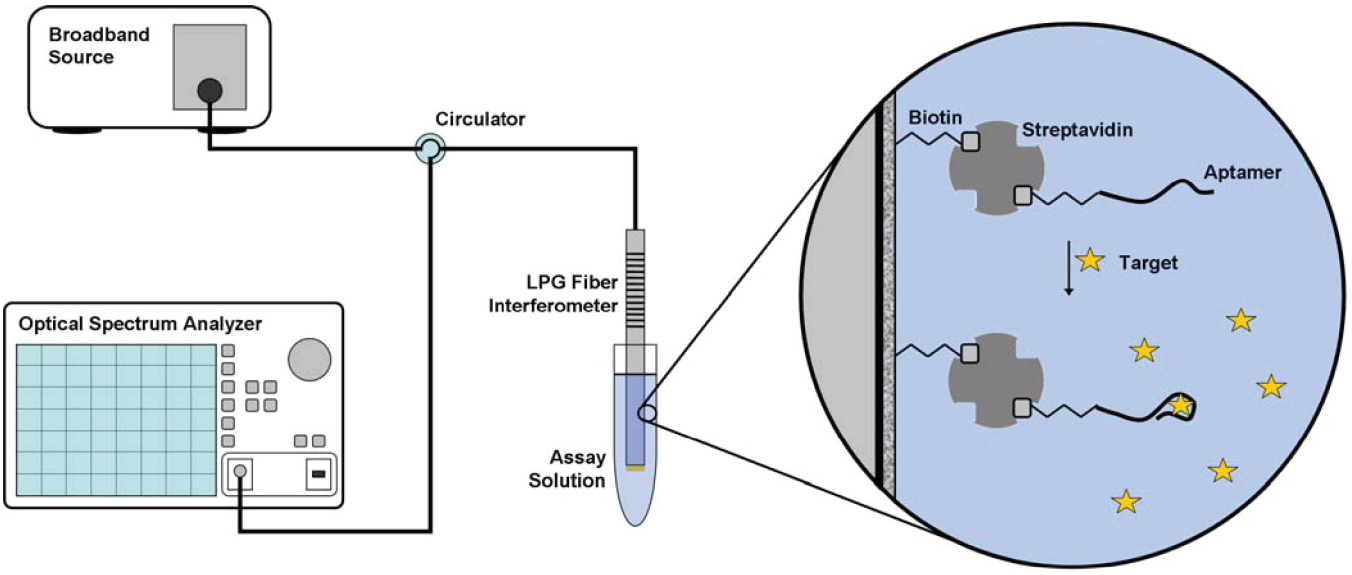

Figure 1. Schematic representation of the experimental configuration for the characterization of the in-fiber interferometer LPG sensor and the analyte detection assay. A broadband light source is transferred by a circulator to the long-period grating fiber sensor and reflected back by a gold mirror on the distal end to an optical spectrum analyzer for recording spectra. The fiber interferometer arm can be coated with a sol−gel derived film and deposited in functionalization or assay solutions to bind the sensing biomolecules for eventual small molecule detection.

films that were dipcast on small silicon wafers (~5 × 15 mm). The silicon wafers were first cleaned and oxidized using piranha solution (Caution: handle in a fumehood with appropriate safety apparel), dipcast in the sols (with or without AuNP) at the same rate as fibers in order to coat half the wafer, and allowed to air-dry. Ellipsometry was performed on a Faraday-modulated self-nulling Exacta 2000 ellipsometer, using light with a wavelength of 632.8 nm and an angle of incidence of 70°. Data were iteratively fit to the Drude equations letting both the thickness and refractive index of the sol−gel film be variables in the fit.

Preparation of LPG Fiber Sensors. A long-period grating of 25 mm, with a period of 310 μm, was inscribed in a Corning SMF-28 fiber (JC Optronics Ltd., Hong Kong) by UV photomasking to induce index modulation using an excimer laser (GSI Lumonics IPEX 848) at 248 nm. The voltage and frequency were set to 30 kV and 20 Hz, respectively, in order to obtain energy above 260 mJ.pulse^{-1}. Spectrum evolution during the LPG fabrication process was monitored to ensure adequate reproducibility in its position (1520−1580 nm) and depth (5 dB). The LPG fiber was then cleaved with a precision fiber cleaver and spliced together with the silica-coated fiber to form the in-fiber Michelson interferometer with a total sensor length 65 mm (including the 25 mm LPG and the 40 mm silica-coated fiber).

Functionalization of Sol−Gel Derived Films on Fibers. For aminosilanization, silica-coated fibers were incubated in a solution containing 4% (v/v) APTES in 650 mM acetic acid, then washed with ddH_2O to remove residual APTES. Biotin was conjugated to the surfaces via succinimide ester coupling using a solution containing 30 mM EDC, 60 mM DSC, and 2.4 mM biotin in 100 mM MES buffer (pH 6.8). Samples were again washed with ddH_2O to remove any excess biotin. Streptavidin (SA) was incubated on the silica films at 500 nM in phosphate buffered saline (PBS) followed by washing with this buffer to remove unbound protein.

Immobilization of DNA Aptamer Complexes. Functionalized film-coated fibers were suspended in the aptamer assay buffer (20 mM Tris buffer at pH 7.8 with 100 mM NaCl and 5 mM $MgCl_2$) containing 100 nM of the biotinylated aptamer at room temperature in order to immobilize the DNA aptamers onto these surfaces. To create the bipartite complex for indirect target-binding studies, the fibers with immobilized aptamer were suspended in assay buffer containing 300 nM of the quencher strand (QDNA) at room temperature prior to any target-binding studies to ensure annealing and quenching. Analyte binding was tested in assay buffer containing varying concentrations of ATP. Film-coated fibers were washed with assay buffer prior to target-binding assays.

LPG Sensor Measurements. For LPG measurements, 30 mm of the interferometer arm of the LPG sensors were mechanically immersed in the various assay solutions using a Newport Universal Controller/Driver. Reflection spectra were obtained using a JDS Uniphase optical broadband light source that was transferred by a circulator to the fiber and conveyed to an Ando AQ6317 optical spectrum analyzer (OSA) for recording of spectra (Figure 1). Using the highest order cladding mode on our LPG sensors, HE_{18}, the interference fringe had a central wavelength between 1560 - 1570 nm with a notch depth of approximately 25 dB, as seen in the full interference spectrum in Figure 2. All LPG interference measurements were performed at room temperature and are reported as a shift in wavelength with a resolution of 0.01 nm.

The wavelength shifts were compared between three types of fiber sensors: the bare fiber, undoped sol−gel derived film-coated fibers, and AuNP-doped sol−gel derived film-coated fibers. In each case, spectra were measured during functionalization every 15 min for the first 6 h and then every 30 min over the next 4 h (600 min total). Aptamer-analyte binding was measured over a period of 120 min (using 1 min intervals for the first 10 min, 2 min for the following 10 and 10 min intervals until 120 min) for both direct and indirect detection of analyte binding and selectivity. For direct measurements, ATP was added to an aptamer-coated fiber, while for indirect measurements, QDNA

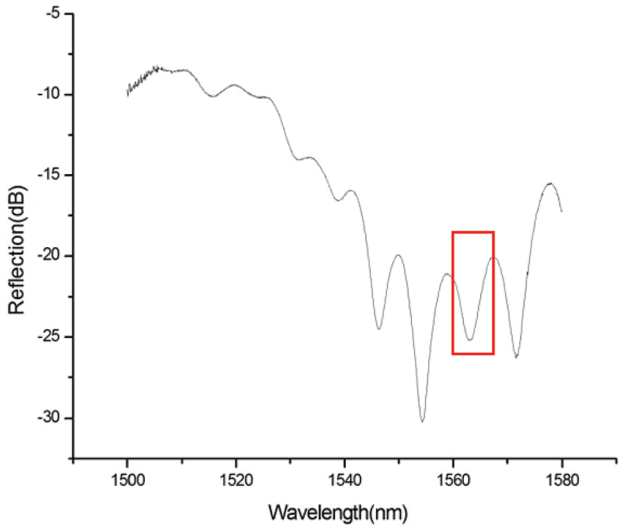

Figure 2. Representative interference spectrum including the interference pattern within the long-period grating (LPG) attenuation envelope. The red box indicates the wavelength shift measurement region between 1560−1570 nm.

was first hybridized to the aptamer using a 3:1 molar ratio of QDNA:aptamer, prior to addition of ATP. Reported measurements represent the average of four individual experiments from separate fibers with typically less than 10% variability. Representative "before and after" interferograms of the functionalization procedures and detection assays can be seen in the Supporting Information, Figures S1−S6, respectively.

RESULTS AND DISCUSSION

Numerical Simulations. Prior to performing experiments, numerical simulations were performed to determine the effect of adding a high RI overlay on the sensitivity of the LPG fiber sensor,[37] as other parameters that can affect sensitivity such as the interferometer length, immersion depth and the group index of the core and cladding modes were kept constant. In the simulation, the radius of the fiber core and cladding were set to 4.15 and 62.5 μm, respectively, while the RI of the fiber core and cladding were set to 1.448933 and 1.440240, respectively.[9] The overlay thickness was fixed at 250 nm, which was the thickness of our silica films as measured by ellipsometry. The effective index as a function of the ambient refractive index is demonstrated using overlay films with different refractive indices (see Figure S7, Supporting Information). The simulation demonstrates that the bare fiber device has relatively poor sensitivity over the ambient RI range from 1.33 (water) to 1.43 (the expected RI of an organic film overlay). However, as the refractive index of the overlay increases, the sensitivity of the LPG sensor also increases. Using an ambient RI of 1.40, about that of the experimental buffer solution, the response of the LPG sensor relative to the bare fiber is about 2-fold greater when the overlay RI is 1.55, 9-fold higher at 1.65 and 14-fold higher at 1.75, respectively. Thus, maximizing the RI of the overlay is crucial for improving the sensitivity of the LPG interferometer response.

Refractive Index Measurements of Macroporous Silica Films. The fabrication of macroporous sol−gel derived silica materials for various applications has recently been reported by our group.[38−40] In the present work, a high surface area silica film, previously fabricated to immobilize fluorescence-reporting aptamers, was utilized to attain both greater biomolecular loading onto the surface of the fiber and to act as a high RI overlayer in order to enhance the LPG interferometer sensitivity. Ellipsometry measurements of this silica film on silicon wafers indicated a RI of 1.34, which simulations predicted would have relatively poor sensitivity. Thus, gold nanoparticles (AuNP) were incorporated into the film material in order to enhance the RI of the film. The RI of the AuNP-doped silica film prior to growth of AuNPs within the film was found to be 1.43. In order to further increase the RI of the silica film layer, the entrapped AuNP were grown, from ∼13 nm mean diameter to ∼25 nm (as determined from the red shift in the absorbance peak to 546 nm), through deposition of additional gold ions upon reduction of Au(III) onto the initial AuNP "seeds" within the silica film. TEM imaging of sol−gel entrapped AuNP grown under identical conditions showed a size range for the particles of 20−40 nm,[21] indicating that a relatively broad distribution of particle sizes is present. The RI of the enlarged AuNP-doped silica film was measured at 1.57, which should provide a greater than 2-fold enhancement in sensitivity, according to our numerical simulations. To verify the sensitivity differences between fibers with different overlay refractive indices, three different fiber configurations were fabricated and compared: (1) unmodified LPG fiber arms, (2) LPG fiber arms coated with a sol−gel derived silica film without added AuNPs, and (3) LPG fiber arms coated with the enlarged AuNP-doped silica film.

Characterization of LPG Fiber Sensor Functionalization. The surface of the fibers was first functionalized with a biotin-streptavidin bridge in order to bind biotinylated structure-switching aptamers for the detection of ATP. The LPG interference fringe wavelength shift was measured during each step of the functionalization procedure in order to ensure binding and detection of each biomolecule: biotin, streptavidin, and the aptamer. As shown in Figure 3, for each species that was immobilized, a blue shift in the spectrum (shift toward shorter wavelength) was observed for all three different fiber types, indicating an increase in ambient RI due to the molecules binding to the fiber surface. The wavelength shifts observed upon binding of biotin were quite small, as expected given the low molecular weight of this species (244 Da). Binding of streptavidin produced a large blue shift in wavelength, corresponding to its large molecular weight (53 kDa), while an intermediate blue shift was observed upon binding of the aptamer (14 kDa). While the expected trend of a higher signal upon binding of a higher molecular weight biomolecule was observed, it is important to note that the relationship between the wavelength shift and the molecular weight is not necessarily linear due to differences in binding concentrations and in the intrinsic structure of the various biomolecules. However, the data presented above clearly indicated that each of the functionalization steps was successful.

A more interesting trend revealed in Figure 3 is the overall amplitude of the wavelength shifts as a function of the RI of the overlay film for each of the different fibers. For all functionalization steps, the bare fiber showed the smallest wavelength shifts, followed by the fiber with the undoped silica film overlay, which generated nearly three times the shift amplitude, and then the fibers with the AuNP-doped silica films, which showed wavelength shifts that were 1.5−2 fold greater than for fibers with undoped silica films, and up to 6-fold greater than were observed for bare LPG fiber arms. The overall enhancements in sensitivity are the result of two factors. The enhanced

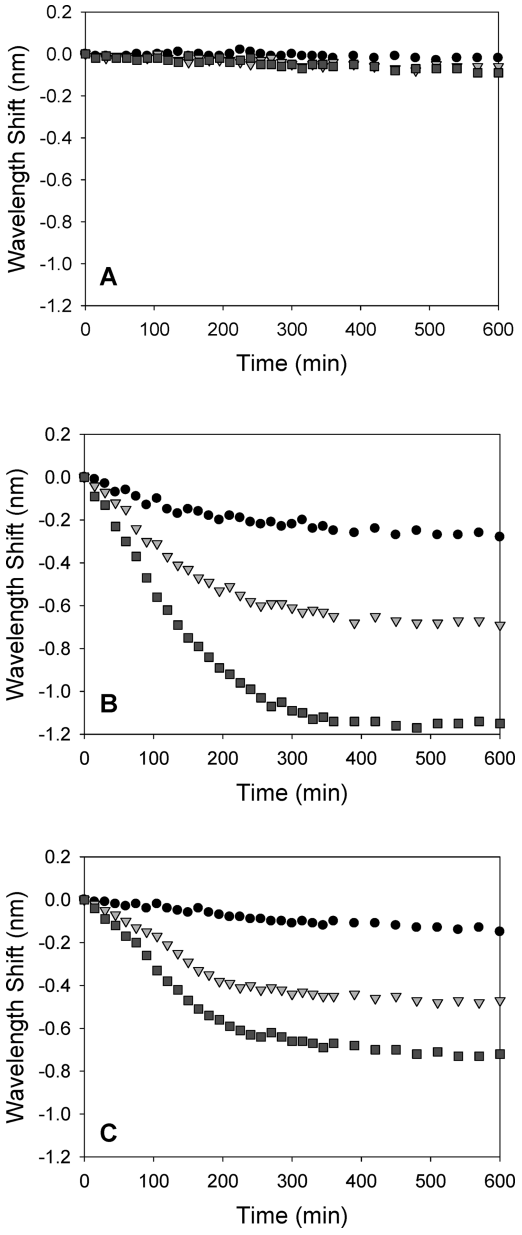

Figure 3. Functionalization of the LPG fiber sensors with sensing biomolecules. Wavelength shifts over time of the three fiber types upon surface-functionalization with (A) biotin, (B) streptavidin, and (C) the ATP-binding aptamer. (●) Bare fiber, (▼) silica-coated fiber, (■) AuNP-doped silica-coated fiber.

sensitivity of the undoped silica-coated fibers relative to the bare fibers is most likely the result of a larger surface area and hence a larger number of molecules bound to the surface (previous studies have shown that such films can immobilize up to 6-fold more aptamer than glass surfaces).[20] The further enhancement of ~2-fold in sensitivity for AuNP doped silica films relative to undoped silica film overlays is due to the higher RI of the AuNP doped films, which is in agreement with the results of the simulations.

In order to demonstrate specific immobilization versus nonspecific binding, streptavidin binding was measured using the enlarged AuNP-doped silica film fibers with and without biotin attached. Over the course of 3 h, no significant change in RI was observed from fibers without bound biotin (Figure S8, Supporting Information).

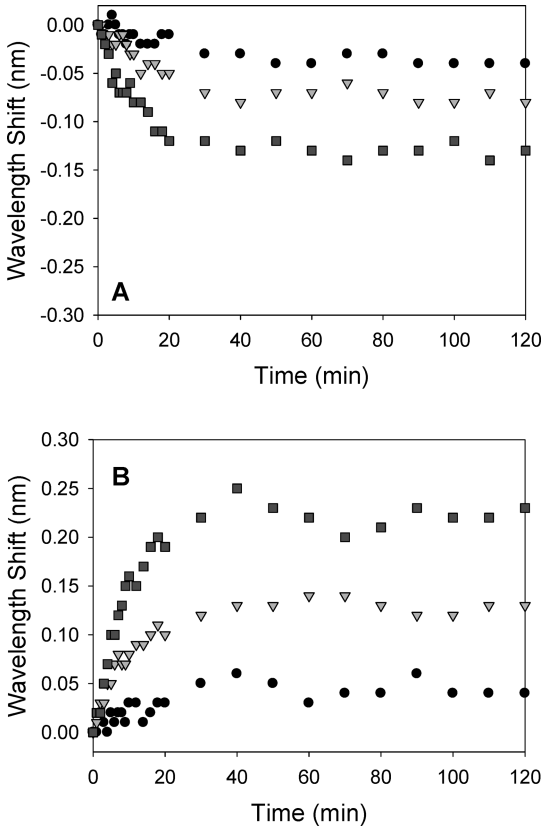

Figure 4. Direct and indirect detection of the small molecule analyte, ATP, using the LPG fiber sensors. Wavelength shift measurements over time for the three fiber types upon (A) direct detection of 1 mM ATP and (B) indirect detection of 1 mM ATP, using the QDNA displacement technique. (●) Bare fiber, (▼) silica-coated fiber, (■) AuNP-doped silica-coated fiber.

Small Molecule Detection using LPG Fiber Sensors. Following aptamer immobilization, each of the three fiber types was assessed for sensitivity to ATP using both the aptamer alone and an aptamer to which QDNA (12 nt plus dabcyl, MW = 4400 Da) had been hybridized. In the first case, the binding of 2 ATP molecules (total MW = 1020 Da) per aptamer would be expected to produce a blue shift in wavelength, while in the latter case the binding should result in displacement of QDNA and a net loss of mass from the surface, producing a red shift in wavelength. Addition of ATP to the LPG interferometer arm with the aptamer alone at a concentration of 1 mM caused the expected blue shift in wavelength, as shown in Figure 4A. It is important to note that the signal change is relatively small due to the low molecular weight of the small molecule analyte, ATP. In the case of ATP binding to the bare fiber, the signal is just above the detection limit of the OSA (ca. −0.03 nm shift). Use of the undoped silica film overlay produced a 2-fold enhancement in the signal, whereas the AuNP doped film resulted in an overall signal enhancement of almost 5-fold relative to the bare fiber. These results clearly show the utility of using high surface area, high RI overlays for sensing of small molecules.

In order to further increase the change in RI observed upon target binding, and to provide an inversion in the signal as a method to reduce the effects of nonspecific binding on the signal,

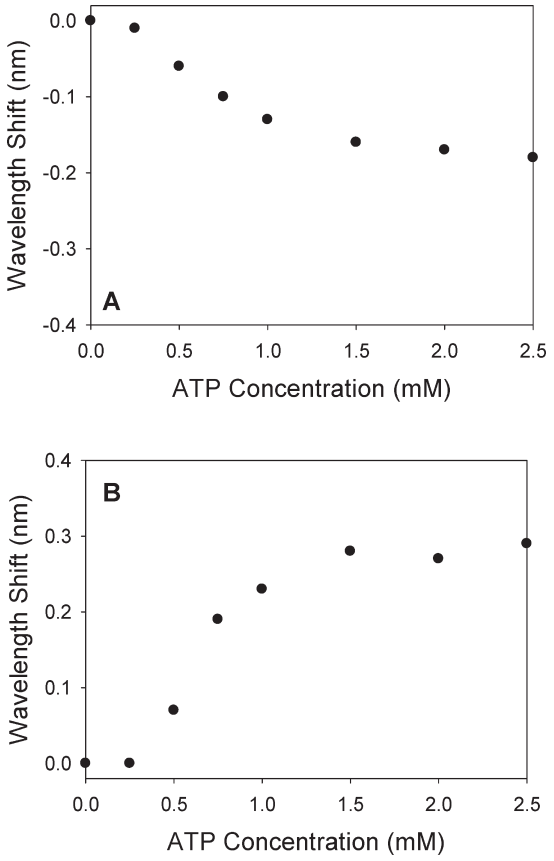

Figure 5. Sensitivity of the ATP aptamer immobilized on the AuNP-doped silica-coated LPG fiber sensor. Response curves of the ATP aptamer immobilized on the AuNP-doped silica-coated LPG fiber sensors to varying concentrations of ATP using (A) direct binding of ATP and (B) indirect detection using QDNA displacement upon ATP binding.

a DNA strand displacement strategy was tested. The complementary QDNA strand was originally created to contain a quencher moiety in order to allow a dequenching mechanism to occur for signal generation in the fluorescence signaling construct of the structure-switching aptamer.[31] As such, this dabcyl-labeled oligonucleotide, termed the "QDNA" strand, was used in this work.

Prior to testing the response of the QDNA system to ATP, the LPG sensor was used to measure the wavelength shift upon hybridization of QDNA to the aptamer. As expected, a shift to a shorter wavelength was observed from all three different fiber types, as the QDNA bound to the fiber surface by hybridization to the aptamer (Figure S9, Supporting Information). To confirm that the binding of the QDNA was due to hybridization, a noncomplementary QDNA strand (for the thrombin binding aptamer) was added; no wavelength shift was observed in this case (Figure S10, Supporting Information). Following QDNA hybridization, 1 mM ATP was added to the LPG interferometer arm and the change in wavelength was recorded. As shown in Figure 4B, the addition of ATP resulted in a shift to a longer wavelength for all fiber types, demonstrating that the binding of two ATP molecules and the displacement of the QDNA strand led to a net loss in mass, and decrease in RI, at the surface. Comparing signal differences between the three different fiber types, it was once again observed that silica coated LPG sensors were ~2.5-fold more sensitive that bare fibers, while AuNP doped films resulted in ~6-fold higher sensitivity relative to bare

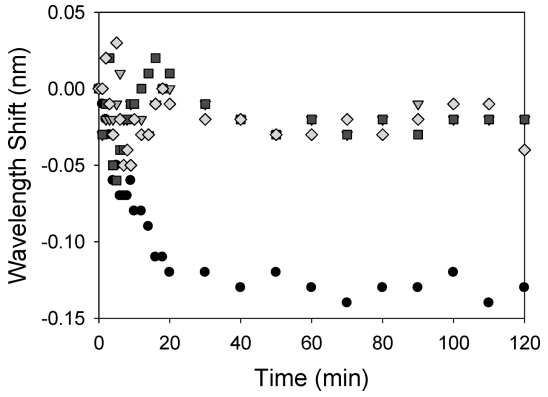

Figure 6. Selectivity of the AuNP-doped silica-coated LPG fiber-immobilized ATP aptamer. Response comparison of the ATP aptamer immobilized on the AuNP-doped silica-coated LPG fiber sensors to different nucleotides using direct analyte detection: (●) 1 mM ATP, (▼) 1 mM CTP, (■) 1 mM GTP and (◆) 1 mM UTP.

fibers. More importantly, the displacement method resulted in a sensitivity improvement of 2-fold relative to direct measurements of ATP, regardless of fiber type. In addition, the strand displacement method provided the expected signal inversion, which should add an additional level of selectivity, as binding of nontarget molecules should not be able to displace the QDNA strand, and would thus produce a blue shift in wavelength rather than a red shift.

Sensitivity and Selectivity of Immobilized Aptamers on LPG Fiber Sensors. In order to further assess the sensitivity of the AuNP-doped film LPG fiber sensors, the shift in wavelength was measured upon addition of various concentrations of ATP. Figure 5 demonstrates the concentration-dependent signal change for both the direct (ATP only) and indirect (QDNA displacement with ATP) methods of target detection, using the AuNP-doped silica film LPG sensor. Both LPG fiber-based detection methods demonstrated similar dynamic ranges and only slightly higher detection limits, of about 400 μM, relative to the original fluorescence-reporting structure-switching ATP aptamer.[31] However, measuring ATP binding using the QDNA displacement provided greater sensitivity for all concentrations tested (double that of direct ATP detection). An important point to note is that the shape of the response curve for the LPG is similar to that obtained using fluorescence measurements, suggesting that the wavelength shift has a linear dependence on RI. This is expected given the small shifts in wavelength (<0.3 nm) that were measured during the binding of ATP.

Selectivity of the ATP aptamer, which is known to bind adenosine derivatives to different degrees but not other nucleotides,[31] was maintained after immobilization onto and detection using the AuNP-doped silica-coated LPG fiber sensors, as the introduction of other nucleotides (CTP, GTP or UTP) at 1 mM produced little or no change in signal using direct analyte detection (Figure 6).

LPG Fiber Sensor Reproducibility and Regeneration. Small variations in the wavelength shifts measured in this study were observed even after apparent stability of the ambient RI in the vicinity of the fiber cladding, though these were never greater than 10% RSD (Figures 4−6 show typical variability in signals of ±0.02 nm). By using an in-fiber interferometer design in which the LPG section of the fiber was excluded from the assay solution, as in this work, the changes in the RI of this medium should not influence the LPG spectrum itself but only shift the interference fringes within the spectrum.[12] Therefore, reproducibility in the

dx.doi.org/10.1021/ac2020432 |*Anal. Chem.* 2011, 83, 7984–7991

fabrication of the LPG, which may influence the initial position of the interference fringes, should not affect the relative wavelength shifts measured due to changes in ambient RI. However, the Michelson interferometer LPG sensing scheme is still sensitive to fluctuations in temperature and vibrations.[13] Thus, minimizing these environmental influences (by temperature control, vibration isolation, etc.) should minimize the observed variability and perhaps improve the detection limits for the analyte by decreasing the inherent error in the baseline measurements. However, the sensitivity and dynamic range of the system depends mostly on the dissociation constant and concentration−response range of the molecular recognition element used, in this case, the QDNA−aptamer complex. The fact that the aptamer defines the sensitivity and dynamic range means that calibration of single fibers from a batch of fibers that were processed similarly should be possible, provided that all fibers have similar coatings and amounts of bound aptamer. Our studies show that fibers have <10% variability, making this calibration method viable.

Although these LPG sensors were intended for and functioned as one-time-use devices, regeneration of the LPG fiber sensors using the QDNA displacement design is possible by reincubation with QDNA for hybridization to the ATP-binding aptamer, as demonstrated in a previous study performed in microwell plates.[20]

CONCLUSIONS

This is the first study to investigate the use of macroporous silica thin films as high RI substrates for the immobilization of DNA aptamers on LPG fiber interferometers and the detection of small molecule analytes using these sensor systems. This study demonstrates that the AuNP-doped silica films contribute a dual functionality: they not only act as a suitable substrate for the high-density immobilization of functional structure-switching aptamers onto the fiber surface but also act as a high RI layer to improve the sensitivity of the LPG sensor itself, through the incorporation of colloidal gold in the film. Furthermore, by utilizing structure-switching aptamers that couple target binding to the displacement of a DNA oligonucleotide strand, the sensitivity is further enhanced due to a larger change in RI. Importantly, this approach also prevents false positive signaling since strand displacement results in a signal that is opposite to that which would result from nonspecific binding, and is specific to the aptamer structure-switching process.

The current LPG sensor design may be further improved by assessing other metal particles as dopants in the silica film, using silica films with even higher surface area, or by designing much larger DNA displacement strands, potentially with metal nanoparticles in place of quenchers, to produce a very large loss of mass upon binding of a small molecule. This strategy can also be extended to other structure-switching aptamer systems for sensitive and specific detection of a range of analytes by the LPG method.

ASSOCIATED CONTENT

Supporting Information. Additional material as noted in the text. This material is available free of charge via the Internet at http://pubs.acs.org.

AUTHOR INFORMATION

Corresponding Author

*Phone: +1-905-525-9140 x27033. Fax: +1-905-527-9950. E-mail: brennanj@mcmaster.ca.

ACKNOWLEDGMENT

C.C. and Y.X. contributed equally to this work. We thank the Natural Sciences and Engineering Research Council of Canada (NSERC) for funding this work. The authors also thank the Canada Foundation for Innovation and the Ontario Innovation Trust for support of this work. Y.L. holds the Canada Research Chair in Directed Evolution of Nucleic Acids. J.D.B. holds the Canada Research Chair in Bioanalytical Chemistry.

REFERENCES

(1) Gauglitz, G. *Anal. Bioanal. Chem.* **2010**, *398*, 2363–2372.
(2) Rapp, B. E.; Gruhl, F. J.; Lange, K. *Anal. Bioanal. Chem.* **2010**, *398*, 2403–2412.
(3) Daghestani, H. N.; Day, B. W. *Sensors* **2010**, *10*, 9630–9646.
(4) Chryssis, A. N.; Saini, S. S.; Lee, S. M.; Hyunmin, Y.; Bentley, W. E.; Dagenais, M. *IEEE J. Sel. Top. Quantum Electron.* **2005**, *11*, 864–872.
(5) Lowder, T. L.; Gordon, J. D.; Schultz, S. M.; Selfridge, R. H. *Opt. Lett.* **2007**, *32*, 2523–2525.
(6) Saini, S. S.; Stanford, C.; Lee, S. M.; Park, J.; DeShong, P.; Bentley, W. E.; Dagenais, M. *IEEE Photonics Technol. Lett.* **2007**, *19*, 1341–1343.
(7) DeLisa, M. P.; Zhang, Z.; Shiloach, M.; Pilevar, S.; Davis, C. C.; Sirkis, J. S.; Bentley, W. E. *Anal. Chem.* **2000**, *72*, 2895–2900.
(8) Rindorf, L.; Jensen, J. B.; Dufva, M.; Pedersen, L. H.; Høiby, P. E.; Bang, O. *Opt. Express* **2006**, *14*, 8224–8231.
(9) Yang, J.; Sandhu, P.; Liang, W. G.; Xu, C. Q.; Li, Y. F. *IEEE J. Sel. Top. Quantum Electron.* **2007**, *13*, 1691–1696.
(10) Bhatia, V.; Vengsarkar, A. M. *Opt. Lett.* **1996**, *21*, 692–694.
(11) James, S. W.; Tatam, R. P. *Meas. Sci. Technol.* **2003**, *14*, R49–R61.
(12) Kim, D. W.; Zhang, Y.; Cooper, K. L.; Wang, A. *Appl. Opt.* **2005**, *44*, 5368–5373.
(13) Swart, P. L. *Meas. Sci. Technol.* **2004**, *15*, 1576.
(14) Shu, X.; Zhang, L.; Bennion, I. *J. Lightwave Technol.* **2002**, *20*, 255.
(15) Yang, J.; Yang, L.; Xu, C. Q.; Li, Y. *J. Lightwave Technol.* **2007**, *25*, 372–380.
(16) Rees, N. D.; James, S. W.; Tatam, R. P.; Ashwell, G. J. *Opt. Lett.* **2002**, *27*, 686–688.
(17) Sandhu, P.; Yang, J.; Xu, C. Q. *IEEE J. Sel. Top. Quantum Electron.* **2010**, *16*, 685–690.
(18) Davies, E.; Viitala, R.; Salomaki, M.; Areva, S.; Zhang, L.; Bennion, I. *J. Opt. A: Pure Appl. Opt.* **2009**, *11*, 1–6.
(19) Du, J.; Cipot-Wechsler, J.; Lobez, J. M.; Loock, H. P.; Crudden, C. M. *Small* **2010**, *6*, 1168–1172.
(20) Carrasquilla, C.; Li, Y.; Brennan, J. D. *Anal. Chem.* **2011**, *83*, 957–965.
(21) Luckham, R. E.; Brennan, J. D. *Analyst* **2010**, *135*, 2028–2035.
(22) Navani, N. K.; Li, Y. F. *Curr. Opin. Chem. Biol.* **2006**, *10*, 272–281.
(23) Shangguan, D.; Li, Y.; Tang, Z.; Cao, Z. C.; Chen, H. W.; Mallikaratchy, P.; Sefah, K.; Yang, C. J.; Tan, W. *Proc. Natl. Acad. Sci. U. S. A.* **2006**, *103*, 11838–11843.
(24) Wilson, D. S.; Szostak, J. W. *Annu. Rev. Biochem.* **1999**, *68*, 611–647.
(25) Famulok, M.; Mayer, G.; Blind, M. *Acc. Chem. Res.* **2000**, *33*, 591–599.
(26) Liu, J.; Cao, Z.; Lu, Y. *Chem. Rev.* **2009**, *109*, 1948–1998.
(27) Bardo, A. M.; Collinson, M. M.; Higgins, D. A. *Chem. Mater.* **2001**, *13*, 2713–2721.
(28) Goring, G. L. G.; Brennan, J. D. *J. Mater. Chem.* **2002**, *12*, 3400–3406.
(29) Jordan, J. D.; Dunbar, R. A.; Bright, F. V. *Anal. Chim. Acta* **1996**, *332*, 83–91.
(30) Martin-Brown, S. A.; Fu, Y.; Saroja, G.; Collinson, M. M.; Higgins, D. A. *Anal. Chem.* **2005**, *77*, 486–494.

(31) Nutiu, R.; Li, Y. F. *J. Am. Chem. Soc.* **2003**, *125*, 4771–4778.
(32) Frens, G. *Nat. Phys. Sci.* **1973**, *241*, 20–22.
(33) Grabar, K. C.; Freeman, R. G.; Hommer, M. B.; Natan, M. J. *Anal. Chem.* **1995**, *67*, 735–743.
(34) Hill, H. D.; Mirkin, C. A. *Nat. Protoc.* **2006**, *1*, 324–336.
(35) Wilcoxon, J. *J. Phys. Chem. B* **2009**, *113*, 2647–2656.
(36) Rupcich, N.; Nutiu, R.; Li, Y. F.; Brennan, J. D. *Anal. Chem.* **2005**, *77*, 4300–4307.
(37) Yang, J.; Yang, L.; Xu, C. Q.; Xu, C.; Huang, W.; Li, Y. *Appl. Opt.* **2006**, *45*, 6142–6147.
(38) Besanger, T. R.; Hodgson, R. J.; Guillon, D.; Brennan, J. D. *Anal. Chim. Acta* **2006**, *561*, 107–118.
(39) Besanger, T. R.; Hodgson, R. J.; Green, J. R.; Brennan, J. D. *Anal. Chim. Acta* **2006**, *564*, 106–115.
(40) Hodgson, R. J.; Chen, Y.; Zhang, Z.; Tleugabulova, D.; Long, H.; Zhao, X. M.; Organ, M.; Brook, M. A.; Brennan, J. D. *Anal. Chem.* **2004**, *76*, 2780–2790.